



Published in final edited form as:

*J Biomed Mater Res A*. 2017 August ; 105(8): 2162–2170. doi:10.1002/jbm.a.36078.

## Development of hybrid scaffolds with natural extracellular matrix deposited within synthetic polymeric fibers<sup>3</sup>

Ritu Goyal<sup>2</sup>, Maria E. Vega<sup>1</sup>, Alexandra K. Pastino<sup>1</sup>, Shivani Singh<sup>1</sup>, Murat Guvendiren<sup>2,3</sup>, Joachim Kohn<sup>2</sup>, N. Sanjeeva Murthy<sup>2</sup>, and Jean E. Schwarzbauer<sup>1,\*</sup>

<sup>1</sup>Department of Molecular Biology, Princeton University, Princeton, NJ 08544-1014 USA

<sup>2</sup>New Jersey Center for Biomaterials, Rutgers University, Piscataway, NJ 08854-8009 USA

<sup>3</sup>Otto H. York Dept. of Chemical, Biological and Environmental Engineering, New Jersey Institute of Technology, Newark NJ 07102

### Abstract

A major challenge of tissue engineering is to generate materials that combine bioactivity with stability in a form that captures the robust nature of native tissues. Here we describe a procedure to fabricate a novel hybrid extracellular matrix (ECM) – synthetic scaffold biomaterial by cell-mediated deposition of ECM within an electrospun fiber mat. Synthetic polymer fiber mats were fabricated using poly(desamino tyrosyl-tyrosine carbonate) (PDTEC) co-spun with poly(ethylene glycol) (PEG) used as a sacrificial polymer. PEG removal increased the overall mat porosity and produced a mat with a layered structure that could be peeled into separate sheets of about 50  $\mu\text{m}$  in thickness. Individual layers had pore sizes and wettability that facilitated cell infiltration over the depth of the scaffold. Confocal microscopy showed the formation of a highly inter-penetrated network of cells, fibronectin fibrils, and synthetic fibers mimicking a complex ECM as observed within tissues. Decellularization did not perturb the structure of the matrix or the fiber mat. The resulting hybrid ECM-scaffold promoted cell adhesion and spreading and stimulated new ECM assembly by stem cells and tumor cells. These results identify a new technique for fabricating highly porous synthetic fibrous scaffolds and an approach to supplement them with natural biomimetic cues.

### Keywords

Synthetic polymer; electrospun fiber mats; decellularization; extracellular matrix (ECM); hybrid scaffold

---

\*Corresponding author: Ph: (609) 258-2893, FAX: (609) 258-1035, jschwarz@princeton.edu.

### Supporting Information

Four figures are included in the Supporting Information. Figures S1 and S2 show NMR spectra and DSC scans from the characterization of residual PEG after washing the fiber mat. Figures S3 shows the reproducibility of cell culture in fiber mats. Figure S4 shows the difference in ECM deposition by tumor cells on a fiber mat compared to a hybrid ECM-scaffold.

## Introduction

Extracellular matrix (ECM) derived from decellularized tissues has been widely explored as a source of biological scaffolds in tissue engineering and regenerative medicine.<sup>1,2</sup> The ECM is a network of polymerized collagens, fibronectin and other proteins and proteoglycans.<sup>3</sup> The versatility of the ECM lies in its ability to modulate cell functions and provide supporting structures for cells. Decellularized ECMs derived from cultured cells have potential as scaffold materials because they provide a three-dimensional architecture composed of natural components that promote cell migration and differentiation.<sup>4-7</sup> Despite these benefits, natural ECM scaffolds are fragile and can be disrupted when cells adhere and apply cell-generated tension. Synthetic fibers, on the other hand, are thicker and stronger than ECM fibrils and can be routinely produced to have reproducible mechanical and material properties. However, they lack the bioactivity of natural ECM, and often result in fibrous encapsulation following implantation.<sup>8</sup> Combining a synthetic material with a natural ECM will capture the advantages of both classes of materials, and produce scaffolds in which mechanical and material properties can be controlled by the choice of the synthetic component and the bioactivity can be controlled by the choice of the cells used to deposit the ECM.

Electrospinning is used extensively to produce nano- and micro-fibers to fabricate scaffolds in tissue engineering and regenerative medicine.<sup>9</sup> The technique can be applied to a variety of polymers to produce fibers with a range of diameters and spatial orientation resulting in fiber mats with very different architectures.<sup>10</sup> Electrospun constructs seeded with cells have been used as scaffolds to engineer tissues such as skin<sup>11</sup>, cornea<sup>12</sup> and neural tissue.<sup>13</sup> Pore size and distribution are important criteria in developing strategies for the design and fabrication of these scaffolds.<sup>14</sup> Porosity in electrospun mats can be increased by salt/polymer leaching,<sup>15,16</sup> using ice crystals,<sup>17</sup> wet electrospinning,<sup>18</sup> laser ablation,<sup>19</sup> combining micro- and nano-fibers<sup>20</sup> and by varying electric field.<sup>21</sup> Large pore sizes and high porosity might compromise the mechanical strength of some scaffolds.<sup>22</sup> However, larger pores are required in scaffolds for cell infiltration and vascularization.<sup>23</sup> Although there is still some controversy about the optimum pore size, it is generally accepted that pore sizes of 50 – 300  $\mu\text{m}$  are necessary to promote cellular infiltration.<sup>24,25</sup> Smaller pores are desirable to transport nutrients, and to serve as a barrier for cellular infiltration, e.g. in skin replacements, wound dressing and endothelium regeneration.<sup>26</sup>

In this study, we explore the use of PEG as a sacrificial polymer to modulate the pore size of electrospun poly(desamino-tyrosyl tyrosine ethyl ester carbonate) (PDTEC), a member of a versatile family of polymers that are readily processable<sup>27</sup> and biocompatible.<sup>28</sup> We used cell culture to show the utility of the electrospun fiber mats for cell infiltration, matrix deposition, and decellularization. Here we show that a hybrid natural ECM-synthetic scaffold promotes new ECM deposition by human stem cells and tumor cells. This hybrid material has beneficial properties of both a natural ECM and synthetic fibers and can be customized to fit a wide array of biomaterials applications.

## Materials and Methods

### Materials

PDTEC was synthesized and characterized for composition, molecular weight (weight average,  $M_w$ ), polydispersity index (PDI), and glass transition temperature ( $T_g$ ) using previously published procedures.<sup>29</sup> Tetrahydrofuran (THF), N,N'-dimethylformamide (DMF) and poly(ethylene glycol) (PEG) 200 kDa were procured from Sigma-Aldrich (USA). PDTEC ( $M_w = 328$  kDa) was dissolved in THF:DMF (9:1) (v/v) and PEG was dissolved in water:ethanol (1:9) (v/v) by stirring at 500 rpm overnight. The solution concentration was optimized to obtain smooth electrospun fibers and a 15% (w/v) solution of each of the polymers was chosen to produce fibers with diameters of 1–2  $\mu\text{m}$ . Molecular weight of PDTEC, determined by gel permeation chromatography<sup>29</sup> was  $328 \pm 10$  kDa (PDI=1.3) before electrospinning, and  $301 \pm 19$  kDa (PDI=1.4) after electrospinning indicating that the polymer remains essentially unchanged during this process.

### Electrospinning

Electrospun fiber mats were prepared in a class 10,000 clean room. The electrospinning device consisted of a syringe pump (World Precision Instruments, USA), high voltage DC power supply, and a rotating mandrel (Reynolds Kitchens, USA, 4.5 cm in diameter, rotating at  $\sim 100$  rpm). Each solution was contained in a 10 mL polyethylene/polypropylene syringe (Norm-Ject, Fisher Scientific, USA). The polymer solution was discharged through a 23-gauge blunt end stainless steel needle (Hamilton Co., USA) at a flow rate of 1 mL/h using the syringe pump; the distance between the tip of the needle and the mandrel was set to 10 cm. The needle was maintained at + 18 kV with respect to grounded mandrel. Smooth fibers were obtained using these parameters. During co-spinning, two needles, one for PEG and the other for PDTEC, connected to their own syringe pumps, were placed either alongside each other, or at  $180^\circ$  from each other to eliminate the possibility of repulsion of the charged jets that could affect the fiber deposition. The fiber mat was built up to  $\sim 150$   $\mu\text{m}$  thick by gradual deposition of 1–2  $\mu\text{m}$  diameter fibers onto a non-stick aluminum sheet wrapped around the mandrel and spun at 100 rpm for 4–5 hr. Fiber mats were dried under vacuum for  $\sim 12$  h at room temperature (RT), and stored in a vacuum desiccator until use.

To visualize the electrospun fibers, the fluorescent dyes rhodamine (red) and Hoechst dye (blue) were added into PDTEC and PEG solutions, respectively. For this experiment, microscope glass slides were attached onto the mandrel using double adhesive tape. The glass slides were detached from the mandrel after the solutions were electrospun for 1 min, and then observed using a fluorescence microscope (Axio Observer D1, Zeiss, Germany) immediately after electrospinning, and after immersion in water for 1 h to remove PEG fibers.

### Fiber morphology

The morphology of the as-spun fiber mats was studied using a scanning electron microscope (SEM; LEO 1550 SEM equipped with Schottky field-emission gun and Robinson backscatter detector) at 20 kV after coating the surfaces with gold-palladium. The  $2 \times 2$  mm specimens were cut from the fiber mats and placed on an aluminum stub (Electron

Microscopy Sciences, USA). Diameters of the fibers were measured from the SEM images using ImageJ software (National Institute of Health, USA) with the average value being calculated from at least 30 measurements from three representative images at 1000× magnification.

### **Proton nuclear magnetic resonance (<sup>1</sup>H-NMR) and differential scanning calorimetry (DSC) analysis**

<sup>1</sup>H-NMR spectra of the fiber mats were obtained using a 500 MHz NMR (Varian, Palo Alto, CA, USA) to quantify the percent of residual PEG after washing. To obtain the NMR spectra, PEG was dissolved in D<sub>2</sub>O and others were dissolved in DMSO-d<sub>6</sub>. DSC scans of the mats were obtained using a Mettler DSC 823e instrument (Mettler Toledo Inc., Columbus OH, USA). The heating rate was 10 °C min<sup>-1</sup>.<sup>30</sup> Heat of fusion was determined from the DSC scans as the area under the melting peak using a base line extending to ~10 °C on either side of the PEG melting peak at 60 °C.

### **Cell culture and matrix decellularization**

PDTEC:PEG co-spun fiber mats were cut into 6 mm squares and each square was placed into a well of a 12-well plate. Squares were washed by immersion and incubation in sterile deionized water for 30 min repeated three times and then incubated in water at 37 °C for 48 h. During the water incubation, layers of the fiber mats started to peel apart and were then carefully separated with forceps (see Figure 1C). Separated layers were transferred to wells of a 24-well plate, washed twice with sterile PBS, and then either used for cell-mediated ECM deposition or stored for use as control scaffolds without ECM. For ECM assembly, 2 × 10<sup>5</sup> NIH 3T3 cells (ATCC, Manassas VA)/well were seeded in DMEM plus 10% bovine calf serum (HyClone Labs, Logan UT). Medium was changed on day 3. For some experiments, medium was supplemented with 50 µg/ml ascorbic acid (Sigma-Aldrich, St. Louis, MO) starting on day 3 and fresh ascorbic acid was then added every other day. Cultures were grown for 7 – 10 days.

Cells in scaffolds were fixed for 15 min in 3.7% formaldehyde in PBS, blocked for 30 min at 37 °C in 5% goat serum, then stained for 30 min at 37 °C with anti-fibronectin polyclonal antiserum (R457)<sup>31</sup> diluted to 1:100 in 2% ovalbumin in PBS followed by incubation with Alexa Fluor® 488-goat anti-rabbit IgG (H+L) diluted to 1:600 (Life Technologies, Carlsbad, CA, USA).<sup>4</sup> Images were captured using a Nikon Eclipse Ti microscope equipped with a Hamamatsu C10600 ORCA-R2 digital camera. Confocal images were captured with the Nikon AI confocal microscope in fluorescence mode. NIS Elements-C software was used to create maximum intensity projections or alpha-blended views of a z-stack (fifty 1 µm stacks) where indicated.

For decellularization, our published protocol<sup>5</sup> was used with the following modification – the second incubation in lysis buffer was for 90 min, 37 °C. Matrices were stored in PBS at 37 °C for at least 48 h before reseeding with cells.

## Analysis of cells on ECM-polymer scaffolds

Human mesenchymal stem cells (MSCs) (Lonza, Allendale NJ) were plated in basal medium on scaffolds with and without ECM at  $2 \times 10^4$  cells/well in a 24-well plate. Human HT1080 fibrosarcoma cells grown in DMEM plus 10% fetal bovine serum (Hyclone) were seeded on scaffolds with and without ECM at  $2 \times 10^5$  cells/well in a 24-well plate. After 24 h, cultures were fixed, permeabilized for 15 min in 0.5% Triton X (Sigma) in PBS, and stained to visualize the decellularized matrix with R457 polyclonal antiserum diluted 1:100, actin cytoskeleton with either rhodamine-phalloidin or Texas Red-X phalloidin (ThermoFisher) 1:50, nuclei with 1  $\mu\text{g/mL}$  DAPI, or newly deposited human fibronectin matrix with HFN7.1 monoclonal anti-fibronectin antibody (DSHB, University of Iowa) diluted at 1:100. Images were captured by epifluorescence or confocal microscopy as indicated.

## Results

### Development of a layered PDTEC:PEG material by co-electrospinning

Electrospun fiber mats made from a single polymer are widely used as substrates for cell culture. However, these mats are usually too dense for the cells to migrate into the core of the fiber mat, and thus, for the most part, serve as 2D substrates. We created a true 3D scaffold by co-spinning PDTEC with PEG used as a sacrificial polymer that can be dissolved away after the electrospinning is complete. This is illustrated in Figure 1 in which fiber mats were prepared by electrospinning for 1 min onto a glass slide. Inclusion of fluorescent dyes, Hoechst for PEG and rhodamine for PDTEC, allowed the visualization of the distributions of the fibers formed from the two polymers (Figure 1A) and the removal of PEG fibers with washing (Figure 1B).

After PEG was removed by washing, the co-spun mats could be separated into layers and peeled apart with forceps into thinner ( $\sim 50 \mu\text{m}$  thick) mats (Figure 1C). No such layering was observed with electrospun mats made with PDTEC alone. This layered structure can be explained as follows. During co-spinning, the polymers from each of the two nozzles are deposited in patches and do not form a comingled continuous mat when the two polymer nozzles are physically situated far apart, in our case  $180^\circ$  around the mandrel. Comingling does not occur even when the two polymer jets are next to each other because the charged jets repel each other, as illustrated in Figure 1D. As a result, in both the arrangements, the PEG and PDTEC patches in the co-spun fiber mat are not physically blended together to form a uniform homogeneous mat. The thickness of the mat decreases slightly upon washing, a small decrease relative to the mass loss (e.g., by  $11 \pm 2\%$  from a starting value  $\sim 115 \mu\text{m}$  compared to a mass loss of 45%). The neighboring PDTEC patches in the washed fiber mat are held together weakly by the PDTEC fibers running between the patches. We speculate that the weak interlayer bonding facilitates the infiltration of cells throughout the thickness of the sheet.

SEM was used to examine fiber morphologies of PDTEC and PDTEC:PEG fiber mats. The co-spun fiber mat had a wide range of fiber diameters including very thin fibers ( $\sim 0.2 \mu\text{m}$  dia.) to fibers with diameters of several  $\mu\text{m}$  (Figure 2B). Very thin fibers were not present in

the PDTEC mat (Figure 2A) or the co-spun mat after removal of PEG (Figure 2C) suggesting that these thin fibers are composed of PEG. PEG fibers could be thinner than PDTEC fibers because of the lower viscosity of the PEG solution.<sup>32</sup> The difference in fiber diameters and densities between unwashed and washed fiber mats (Figures 2B, C) indicate that these thin fibers were dissolved by washing with water, further supporting the contention that these are PEG fibers. A comparison of the masses of the fiber mats before and after washing suggests that there is some residual PEG present in the fiber mat. There was only a 45% weight loss in the 1:1 PDTEC:PEG mat upon PEG removal instead of the expected 50%. Similar results were obtained with a preparation using a 2:1 PDTEC:PEG mat (27 % vs. the expected 33%). The presence of PEG in the washed mat was confirmed by the presence of the PEG peak at  $\delta$  3.4 in <sup>1</sup>H-NMR and by the PEG melting peak at 60 °C in DSC scans (Supplementary Figure S1 and S2, respectively). The calculated residual PEG was ~ 2.3 wt% by NMR, and ~ 2 wt% by DSC. It is most likely that the residual PEG remains as a thin coating on the PDTEC fibers after the co-spun mat is washed.

### Cell culture and matrix deposition within electrospun fiber mats

PDTEC fiber mats after PEG removal were used for deposition of an ECM. Mouse NIH 3T3 fibroblasts attached to the scaffold fibers and assembled a dense matrix that is rich in fibronectin as shown in the maximum intensity projection normal to the surface of confocal images (Figure 3A). The maximum projection of a lateral view (orthogonal to A) shows the depth of cell infiltration into the fiber mat (Figure 3B). This particular fiber mat was ~ 40  $\mu$ m thick. Depth measurements of DNA and fibronectin stains showed that cells and matrix spanned ~35  $\mu$ m within the fiber mat. Thus cells are able to move into the fiber mats and assemble a natural matrix between the scaffold fibers. The perspective view showing volume rendering of the matrix within the scaffold shows the overall density of the matrix and thickness of the fibronectin fibrils and cell nuclei (Figure 3C). This fiber mat preparation procedure is reproducible since cell infiltration and matrix deposition were observed within four independent preparations of PDTEC:PEG fiber mats (Supplementary Figure S3). Using our established procedure<sup>5</sup> to decellularize the matrix, we generated a hybrid material composed of natural ECM within a synthetic fiber mat. Polymer fiber integrity and organization were maintained throughout the decellularization procedure (Figure 4A, B). After decellularization, a dense network of matrix fibrils remained in place between and around the synthetic fibers (Figure 4C, D).

### Cell responses to hybrid ECM-polymer scaffolds

The presence of a natural ECM in a hybrid scaffold material has the potential of introducing novel biological cues that can stimulate specific cell activities. To examine cell behaviors in response to a hybrid ECM-polymer scaffold compared to cells on a polymer scaffold after PEG removal but without ECM, the extent of attachment and spreading of human mesenchymal stem cells (MSCs) on the two scaffolds were analyzed by staining the actin cytoskeleton and the underlying mouse NIH 3T3 fibronectin matrix. Cells on the scaffold alone were spindly as they grew along individual fibers that were only a few microns in diameter at the widest (Figure 5A–C). In contrast, in the hybrid ECM-polymer scaffold, the ECM filled the spaces between synthetic fibers; the fibrils of the underlying ECM are visible between the spread cells and provided many natural cell-binding sites for cell adhesion. As a

result, MSCs were highly spread on the hybrid scaffold with extensive, well-formed actin stress fibers (Figure 5D–F). Confirming the elongated morphology of cells on scaffold alone, the calculated aspect ratios (length/width) of cells spread after one day averaged  $15.0 \pm 5.0$  (n=15). In contrast, on the hybrid ECM-polymer scaffold, aspect ratios averaged  $2.9 \pm 1.6$  (n=13), which is much closer to 1.0 and indicates circumferential cell spreading. In addition to providing adhesion sites and signaling cues for cells, the ECM also increased the surface area of the scaffold thus supporting the adhesion of higher numbers of MSCs (compare Figure 5A and D). These results show that the presence of a natural ECM enhances cell interactions with the PDTEC fiber mat.

Matrix assembly is a key function of MSCs and is an essential part of tissue regeneration. Fibronectin fibrils are the first ECM components assembled by mesenchymal cells and are required for deposition of collagens and other ECM proteins.<sup>6</sup> We therefore analyzed the effect of a hybrid scaffold on this MSC function. Human MSCs were grown on either a hybrid ECM-polymer scaffold or a scaffold alone for 7 days. We did not detect any changes in the synthetic fiber mats after this extended time in culture (Figure 6C, F). To distinguish new human fibronectin matrix assembly from the underlying mouse ECM, a human fibronectin-specific antibody was used for staining. MSCs on the hybrid material were well spread and assembled a significant amount of new fibronectin-rich matrix (Figure 6D,E). As at the shorter (1 d) time point (see Figure 5), the cells on the scaffold alone remained largely spindle-shaped and produced minimal amounts of new matrix (Figure 6A,B). Similar results were obtained with human tumor cells on a hybrid ECM-scaffold compared to a scaffold without ECM (Supplementary Figure S4). Together these results demonstrate the ability of this hybrid natural ECM-synthetic fiber mat scaffold to induce cell shape changes and new matrix production, activities that are essential for tissue repair and regeneration.

## Discussion

A major goal of tissue engineering is to design and produce materials that recreate the functionality of a native tissue. This requires reproducing the structural organization and biological features that control tissue-specific cell behaviors. Because the ECM is a major part of any cell's microenvironment, we developed a hybrid scaffold that combines the biological architecture and components of a natural ECM with the reproducibility and stability of a synthetic material. Our results show that removal of sacrificial fibers from an electrospun PDTEC:PEG fiber mat yields a scaffold whose fiber morphology, fiber distribution, and pore size are conducive to cell infiltration. Cells penetrate the scaffold and, importantly, the PDTEC fiber density is such that cells are able to deposit an ECM that interconnects the fibers forming a truly hybrid natural-synthetic material. We showed that the hybrid ECM-polymer scaffold promotes new ECM assembly by MSCs and tumor cells. This novel material thus has the properties and functionality to support tissue regeneration.

Electrospinning is a versatile method to prepare fiber mats out of a variety of synthetic polymers.<sup>9</sup> However, fiber diameters tend to be much larger than that of the ECM fibers that are present in developing tissues. While nanofibers can be generated by electrospinning, the resulting density and elasticity of fibers in the mat are such that cells are not able to infiltrate making such fiber mats essentially 2D substrates. The fiber mats prepared in this work are

different in that they function as 3D substrates. We speculate that because the PEG and PDTEC fibers are co-spun into a 150  $\mu\text{m}$  thick fiber mat from two different nozzles over an extended period, the fibers are deposited in adjacent or overlapping patches either because of electrostatic repulsion of the charged jets or because of the physical separation of the jets. Upon washing away of the intervening sacrificial PEG fibers, the mat will be an assembly of PDTEC fibers, some of which are only weakly linked because of PEG removal. We propose that the linkages between the PDTEC fibers within a plane are more numerous, and hence stronger, than the interlayer linkages. When peeled apart, we suggest that the fibers tear by following the path of least resistance. Such layered structure was not observed when PDTEC and PEG were dissolved in a common solution and deposited from a single nozzle (unpublished results). This more porous layered structure allowed cells to assemble a natural ECM within the fiber mat rather than on top of it. If PEG is deposited as globules then we would have PDTEC scaffold with large pores. But PEG and PDTEC are both deposited as patches of about the same area and thickness. Thus, removal of the sacrificial PEG results in PDTEC layers (not uniform) that can be separated.

The presence of residual PEG on PDTEC fibers, a hydrophilic coating on a hydrophobic substrate, makes the co-spun fiber mat more wettable than a mat composed of PDTEC alone. However, the amount of PEG left behind is not sufficient to inhibit cell attachment.<sup>33</sup> The wettability would make the mats more receptive to cell attachment during seeding. The 3D structure and high porosity of fiber mats prepared in this way facilitate the migration of cells into the mat where they assemble fibronectin fibrils within and between synthetic fibers to form a highly interpenetrated network that maintains its integrity throughout decellularization. The strength of the synthetic fibers provides a stable environment for the ECM such that the hybrid ECM-polymer scaffolds can be stored for at least several months.<sup>34</sup>

The ECM adds biological elements and properties that are lacking in a simple synthetic fiber scaffold. ECM fibrils contain binding sites for cells and proteins and supply structural cues that determine cell arrangements. In addition, ECM fibrils are more compliant and elastic than the rigid synthetic fibers.<sup>7</sup> This fibril elasticity provides a mechanically appropriate environment that cells respond to by activating mechanosensitive pathways to promote cell functions and tissue growth.<sup>35</sup>

There are several important advantages to our procedure. While many groups have added cell-adhesive molecules to fibrous mats by attaching RGD peptides or coating fibers with solutions of fibronectin or other ECM proteins,<sup>36,37</sup> these treatments do not provide the full benefits of a cell-derived ECM. The natural fibrillar architecture and biophysical properties of the ECM, the many different cell-produced components present within ECM fibrils or associated with them, and the space filling function of the ECM are all missing in the absence of a cell-derived ECM. We have previously shown that NIH 3T3 cells incorporate type I collagen into the ECM<sup>38</sup> and, using mass spectrometry of the decellularized ECM, we have detected other types of collagen, tenascin-C, and proteoglycans among other ECM proteins (unpublished observations). Importantly, the novelty of the hybrid ECM-scaffold is not limited to a single type of ECM or polymer. One can customize it by varying the cells that are used for matrix deposition, changing the polymer for electrospinning, or both.



## Conclusions

We demonstrate that a PDTEC:PEG fiber mat provides a reliable support for cell growth and matrix deposition within the PDTEC scaffold after removal of the PEG sacrificial polymer. The ECM fibrils are stably integrated between and around the synthetic fibers mimicking a connective tissue ECM. Decellularization of the ECM generates a novel hybrid ECM-synthetic scaffold with enhanced functionality compared to the scaffold without ECM by promoting not only cell adhesion but also new ECM assembly. By using fibroblasts, stem cells, immune cells, neural cells, etc., individually or in combination, one can incorporate an ECM that varies in composition and/or organization to match or enhance the tissue type of interest.

## Supplementary Material

Refer to Web version on PubMed Central for supplementary material.

## Acknowledgments

Funding for this work was provided by the National Institutes of Health to RESBIO - The National Resource for Polymeric Biomaterials (P41 EB001046) (to JK) and R01 CA160611 (to JES). We thank Christina O'Halloran for technical assistance. S. Singh was supported by NIH T32 Post-doctoral Training Grant T32EB005583 (to the New Jersey Center for Biomaterials). A. K. Pastino was supported by NIH T32 GM007388 pre-doctoral training grant to the Department of Molecular Biology at Princeton University. M. E. Vega is supported by NRSA fellowship F32 DK109622.

## References

1. Badylak SF, Freytes DO, Gilbert TW. Extracellular matrix as a biological scaffold material: Structure and function. *Acta Biomaterialia*. 2009; 5(1):1–13. [PubMed: 18938117]
2. Hoshiba T, Lu HX, Kawazoe N, Chen GP. Decellularized matrices for tissue engineering. *Expert Opinion on Biological Therapy*. 2010; 10(12):1717–1728. [PubMed: 21058932]
3. Schwarzbauer JE, Desimone DW. Fibronectins, their fibrillogenesis, and in vivo functions. *Cold Spring Harb Perspect Biol*. 2011; 3doi: 10.1101/cshperspect.a005041
4. Engler AJ, Chan M, Boettiger D, Schwarzbauer JE. A novel mode of cell detachment from fibrillar fibronectin matrix under shear. *J Cell Sci*. 2009; 122:1647–1653. [PubMed: 19401337]
5. Mao Y, Schwarzbauer JE. Stimulatory effects of a three-dimensional microenvironment on cell-mediated fibronectin fibrillogenesis. *J Cell Sci*. 2005; 118:4427–4436. [PubMed: 16159961]
6. Singh P, Carraher C, Schwarzbauer JE. Assembly of fibronectin extracellular matrix. *Annu Rev Cell Dev Biol*. 2010; 26:397–419. [PubMed: 20690820]
7. Mao Y, Schwarzbauer JE. Accessibility to the fibronectin synergy site in a 3D matrix regulates engagement of  $\alpha 5\beta 1$  versus  $\alpha v\beta 3$  integrin receptors. *Cell Commun Adhes*. 2006; 13:267–277. [PubMed: 17162669]
8. Rolfe B, Mooney J, Zhang B, Jahnke S, Le S-J, Chau Y-Q, Huang Q, Wang H, Campbell G, Campbell J. The Fibrotic Response to Implanted Biomaterials: Implications for Tissue Engineering. *InTech China: InTech*. 2011:19.
9. Sill TJ, von Recum HA. Electrospinning: applications in drug delivery and tissue engineering. *Biomaterials*. 2008; 29(13):1989–2006. [PubMed: 18281090]
10. Agarwal S, Wendorff JH, Greiner A. Progress in the field of electrospinning for tissue engineering applications. *Adv Mater*. 2009; 21(32–33):3343–3351. [PubMed: 20882501]
11. Zhu X, Cui W, Li X, Jin Y. Electrospun fibrous mats with high porosity as potential scaffolds for skin tissue engineering. *Biomacromolecules*. 2008; 9(7):1795–801. [PubMed: 18578495]

12. Wray LS, Orwin EJ. Recreating the microenvironment of the native cornea for tissue engineering applications. *Tissue Eng Part A*. 2009; 15(7):1463–1472. [PubMed: 19193140]
13. Yang F, Murugan R, Wang S, Ramakrishna S. Electrospinning of nano/micro scale poly(L-lactic acid) aligned fibers and their potential in neural tissue engineering. *Biomaterials*. 2005; 26(15): 2603–10. [PubMed: 15585263]
14. Zhong S, Zhang Y, Lim CT. Fabrication of large pores in electrospun nanofibrous scaffolds for cellular infiltration: a review. *Tissue Eng Part B Rev*. 2012; 18(2):77–87. [PubMed: 21902623]
15. Kim TG, Chung HJ, Park TG. Macroporous and nanofibrous hyaluronic acid/collagen hybrid scaffold fabricated by concurrent electrospinning and deposition/leaching of salt particles. *Acta Biomaterialia*. 2008; 4(6):1611–1619. [PubMed: 18640884]
16. Baker BM, Gee AO, Metter RB, Nathan AS, Marklein RA, Burdick JA, Mauck RL. The potential to improve cell infiltration in composite fiber-aligned electrospun scaffolds by the selective removal of sacrificial fibers. *Biomaterials*. 2008; 29(15):2348–2358. [PubMed: 18313138]
17. Leong MF, Rasheed MZ, Lim TC, Chian KS. In vitro cell infiltration and in vivo cell infiltration and vascularization in a fibrous, highly porous poly(D,L-lactide) scaffold fabricated by cryogenic electrospinning technique. *Journal of Biomedical Materials Research Part A*. 2009; 91A(1):231–240.
18. Yokoyama Y, Hattori S, Yoshikawa C, Yasuda Y, Koyama H, Takato T, Kobayashi H. Novel wet electrospinning system for fabrication of spongiform nanofiber 3-dimensional fabric. *Materials Letters*. 2009; 63(9–10):754–756.
19. Choi HW, Johnson JK, Nam J, Farson DF, Lannutti J. Structuring electrospun polycaprolactone nanofiber tissue scaffolds by femtosecond laser ablation. *Journal of Laser Applications*. 2007; 19(4):225–231.
20. Deitzel JM, Kleinmeyer JD, Hirvonen JK, Tan NCB. Controlled deposition of electrospun poly(ethylene oxide) fibers. *Polymer*. 2001; 42(19):8163–8170.
21. Zhang DM, Chang J. Electrospinning of Three-Dimensional Nanofibrous Tubes with Controllable Architectures. *Nano Letters*. 2008; 8(10):3283–3287. [PubMed: 18767890]
22. Karageorgiou V, Kaplan D. Porosity of 3D biomaterial scaffolds and osteogenesis. *Biomaterials*. 2005; 26(27):5474–91. [PubMed: 15860204]
23. Hofmann S, Hagenmuller H, Koch AM, Muller R, Vunjak-Novakovic G, Kaplan DL, Merkle HP, Meinel L. Control of in vitro tissue-engineered bone-like structures using human mesenchymal stem cells and porous silk scaffolds. *Biomaterials*. 2007; 28(6):1152–62. [PubMed: 17092555]
24. Oh SH, Park IK, Kim JM, Lee JH. In vitro and in vivo characteristics of PCL scaffolds with pore size gradient fabricated by a centrifugation method. *Biomaterials*. 2007; 28(9):1664–71. [PubMed: 17196648]
25. Liu Q, Bergenstock MK. Extra Cellular Matrix and Its Application as Coating on Synthetic 3D Scaffolds for Guided Tissue Regeneration. *Tissue Regeneration: Where Nano-Structure Meets Biology*. 2014; 2:205–217.
26. Macri LK, Sheihet L, Singer AJ, Kohn J, Clark RAF. Ultrafast and fast bioerodible electrospun fiber mats for topical delivery of a hydrophilic peptide. *J Control Release*. 2012; 161(3):813–820. [PubMed: 22580116]
27. Bourke SL, Kohn J. Polymers derived from the amino acid L-tyrosine: polycarbonates, polyarylates and copolymers with poly(ethylene glycol). *Adv Drug Deliv Rev*. 2003; 55:447–466. [PubMed: 12706045]
28. Magno MHR, Kim J, Srinivasan A, McBride S, Bolikal D, Darr A, Hollinger JO, Kohn J. Synthesis, degradation and biocompatibility of tyrosine-derived polycarbonate scaffolds. *J Mater Chem*. 2010; 20(40):8885–8893.
29. Ertel SI, Kohn J. Evaluation of a series of tyrosine-derived polycarbonates as degradable biomaterials. *J Biomed Mater Res Part A*. 1994; 28(8):919–930.
30. Sommerfeld SD, Zhang Z, Costache MC, Vega SL, Kohn J. Enzymatic surface erosion of high tensile strength polycarbonates based on natural phenols. *Biomacromolecules*. 2014; 15(3):830–836. [PubMed: 24432806]

31. Aguirre KM, McCormick RJ, Schwarzbauer JE. Fibronectin self-association is mediated by complementary sites within the amino-terminal one-third of the molecule. *J Biol Chem.* 1994; 269:27863–27868. [PubMed: 7961716]
32. Koski A, Yim K, Shivkumar S. Effect of molecular weight on fibrous PVA produced by electrospinning. *Mater Lett.* 2004; 58(3):493–497.
33. Tziampazis E, Kohn J, Moghe PV. PEG-variant biomaterials as selectively adhesive protein templates: model surfaces for controlled cell adhesion and migration. *Biomaterials.* 2000; 21(5): 511–520. [PubMed: 10674816]
34. Goyal R, Guvendiren M, Freeman O, Mao Y, Kohn J. Optimization of polymer-ECM composite scaffolds for tissue engineering: Effect of cells and culture conditions on polymeric nanofiber mats. *J Funct Biomater.* 2017; 8doi: 10.3390/jfb8010001
35. Mammoto T, Mammoto A, Ingber DE. Mechanobiology and developmental control. *Annu Rev Cell Dev Biol.* 2013; 29:27–61. [PubMed: 24099083]
36. Liu X, Holzwarth JM, Ma PX. Functionalized synthetic biodegradable polymer scaffolds for tissue engineering. *Macromol Biosci.* 2012; 12:911–919. [PubMed: 22396193]
37. Yoo HS, Kim TG, Park TG. Surface-functionalized electrospun nanofibers for tissue engineering and drug delivery. *Adv Drug Deliv Rev.* 2009; 61:1033–1042. [PubMed: 19643152]
38. Singh S, Bandini SB, Donnelly PE, Schwartz J, Schwarzbauer JE. A cell-assembled, spatially aligned extracellular matrix to promote directed tissue development. *J Mater Chem B Mater Biol Med.* 2014; 2:1449–1453. [PubMed: 24707354]

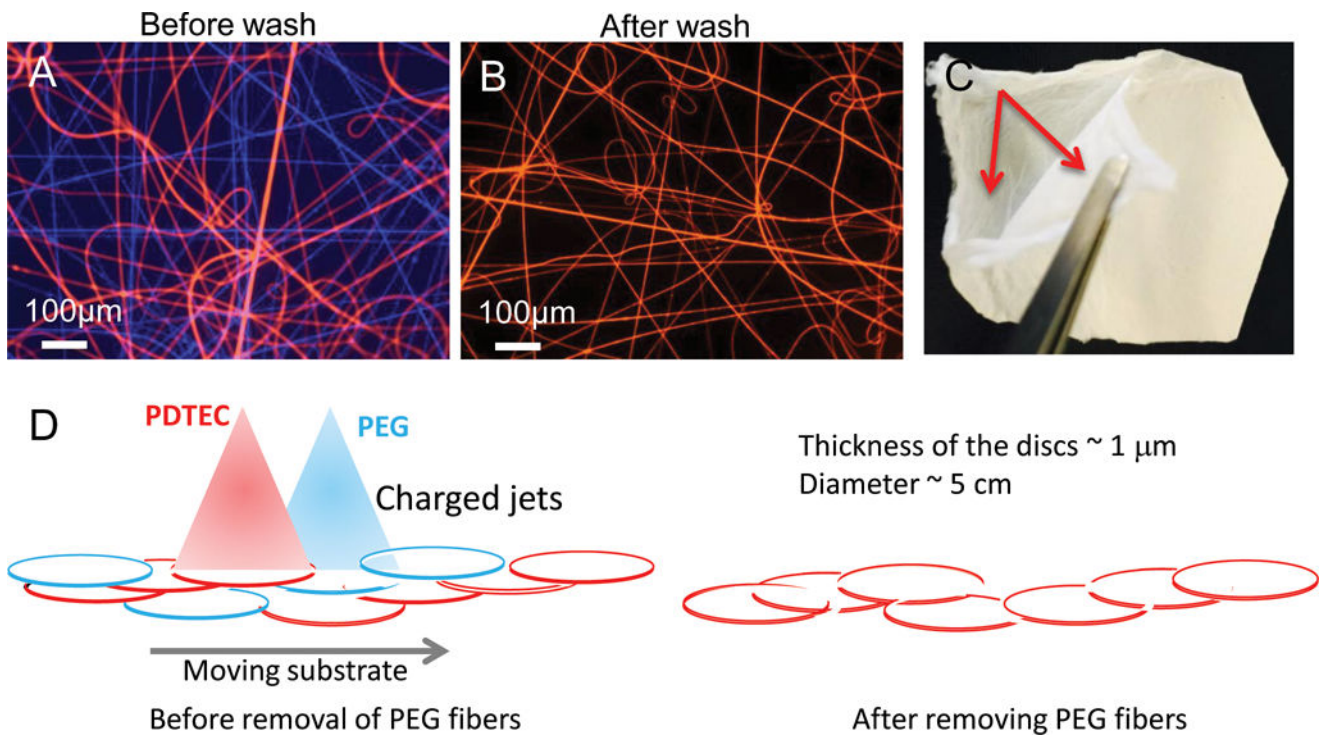


**Figure 1. PDTEC:PEG electrospun fibers before and after PEG removal**

Optical microscopy images of fluorescent-labeled electrospun fibers before (A) and after (B) washing with water to remove PEG fibers. PEG fibers are blue and PDTEC fibers are red. Scale bar = 200  $\mu\text{m}$ . (C) Layered structure in co-spun mat after PEG removal. The arrows point to the two delaminated layers. (D) Schematic of the deposition of PDTEC and PEG to illustrate the formation of a layered structure. For clarity, patches of PEG or PDTEC fibers are shown as discs, and the fibers inside the patches as well as those between them are not shown. In the left diagram, PEG and PDTEC jets with same type of charge repel each other, and are shown depositing separate patches to illustrate weak intermingling of the two polymer fibers. The right diagram shows that upon the dissolution of the PEG segments by washing, weakly interwoven PDTEC discs are left behind.

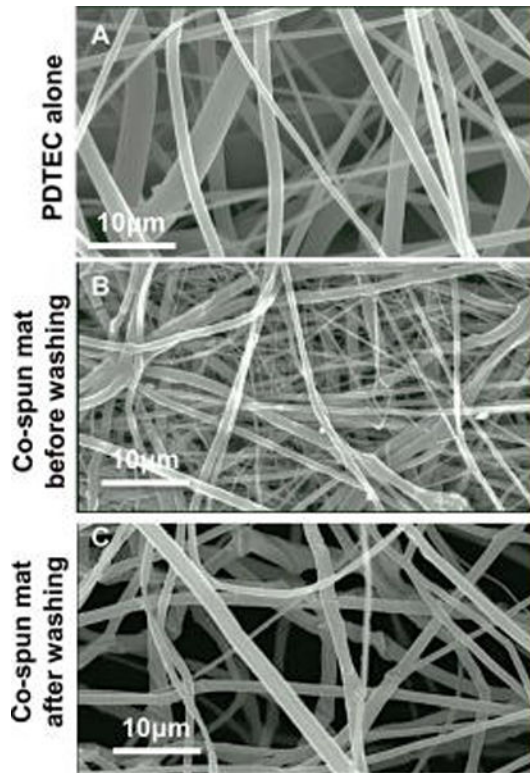


**Figure 2. SEM images of electrospun fiber mats**

(A) Fiber mat from PDTEC by itself. (B) Co-spun PDTEC-PEG mat before washing. (C) Co-spun PDTEC-PEG mat after washing showing the more open structure compared to that in the unwashed mat.

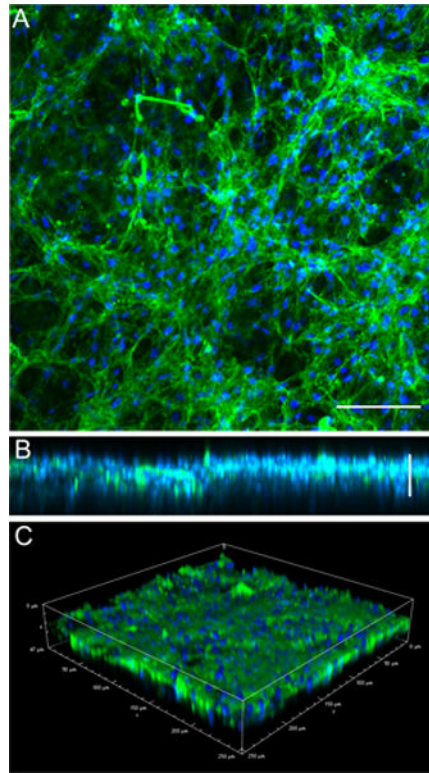


**Figure 3. Cell integration and matrix deposition in a PDTEC:PEG polymer fiber mat**  
PDTEC:PEG polymer fiber mat were washed in dH<sub>2</sub>O to remove PEG. Mouse NIH 3T3 fibroblasts were grown for 7 days within the PDTEC fiber mat. Cells were fixed and stained with R457 anti-fibronectin antiserum (green) and DAPI to stain the nuclei (blue). Confocal images shown are (A) maximum intensity projection (scale bar = 50  $\mu$ m), (B) maximum intensity projection of the view orthogonal to (A) showing the depth of the matrix within the scaffold, and (C) an alpha-blended volume view (scale bar = 25  $\mu$ m).

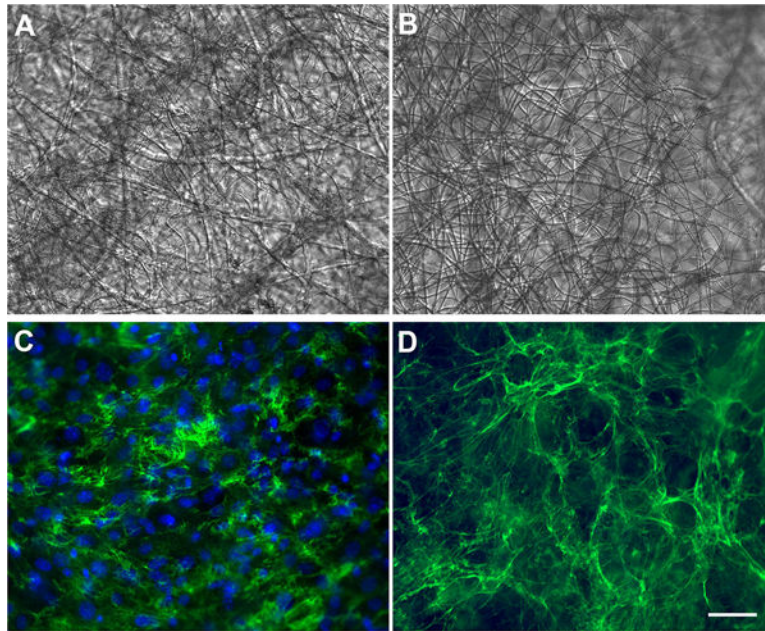


**Figure 4. ECM deposition within PDTEC:PEG scaffolds**

After PEG removal, NIH3T3 cells were cultured within the scaffolds for 7 d and then fixed and stained with anti-fibronectin antibodies (green) and DAPI (blue). A and C are the same microscope field; (A) shows the bright field image of the synthetic fibers and (C) shows the fluorescence signal of matrix and nuclei. In parallel, a similar culture was decellularized and then fixed and stained as above. B and D show the same field by bright field and fluorescence imaging. The fiber mat organization is not affected by the decellularization procedure (compare A and B). The absence of DAPI staining in D shows that cells are removed by decellularization while matrix fibrils remain in place. Scale bars = 50  $\mu\text{m}$ .

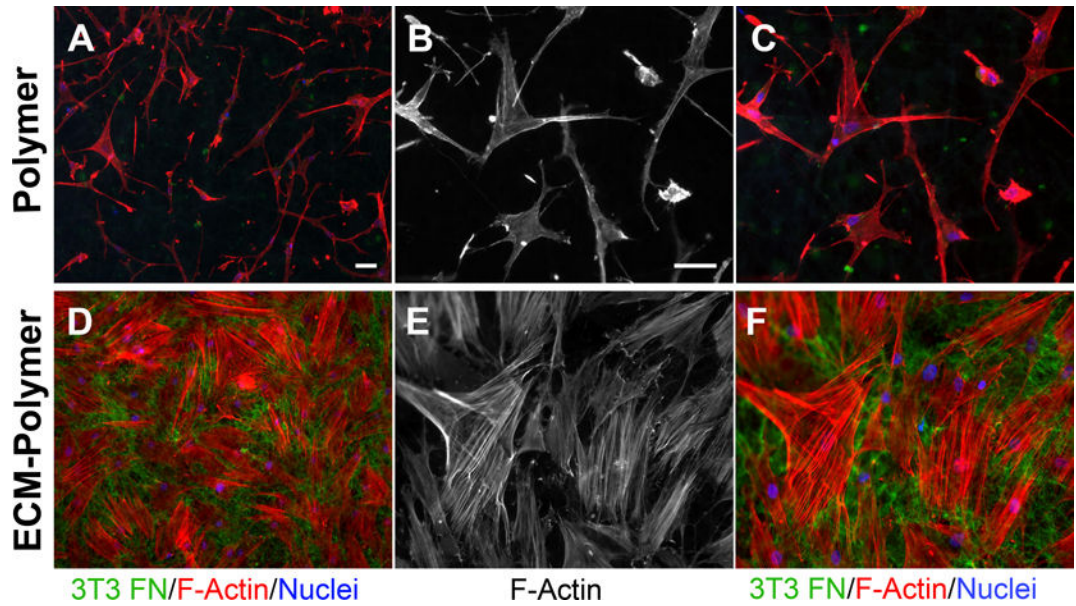


**Figure 5. Adhesion and spreading of MSCs on a hybrid ECM-polymer scaffold**

Human MSCs were plated on a hybrid ECM – polymer scaffold or on a polymer scaffold without ECM. Cells were allowed to spread for 24 h, then cell shapes were visualized by staining actin filaments with rhodamine-phalloidin (red) and DAPI (blue). Samples were also stained with anti-fibronectin antiserum to show the NIH 3T3 matrix within the scaffold. B, C, E, F are higher magnification images of the samples in A and D. Scale bars = 50  $\mu\text{m}$ .



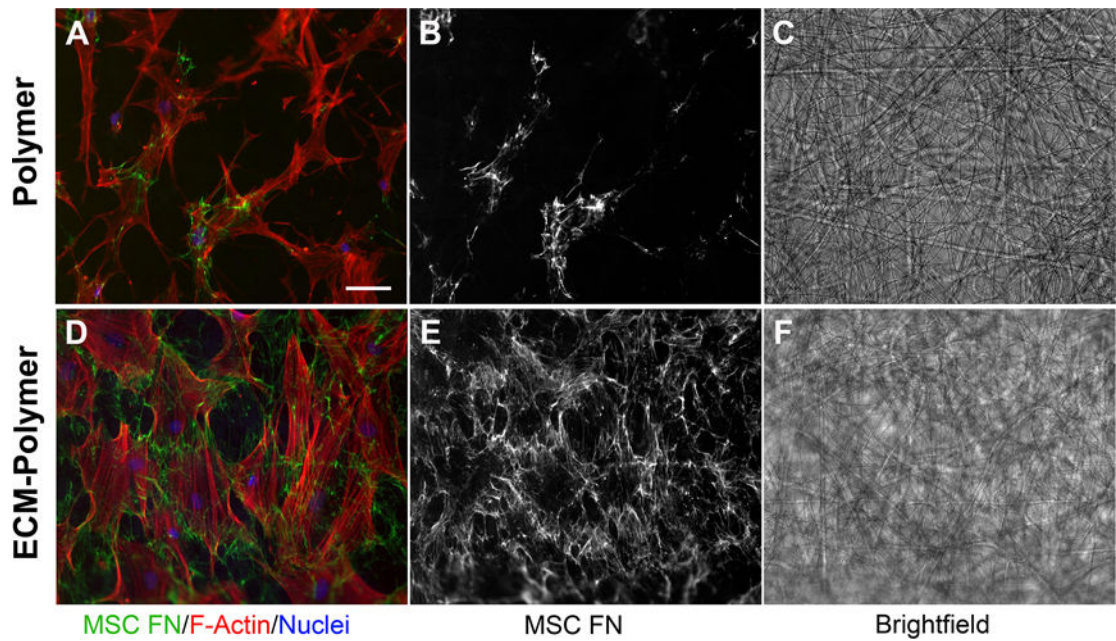


**Figure 6. Matrix assembly by MSCs on a hybrid ECM-polymer scaffold**

Cells were plated as in Figure 5 but then grown for 7 d before staining with rhodamine-phalloidin and DAPI. Human MSC-produced and assembled fibronectin was detected with a human fibronectin-specific monoclonal antibody. Considerably more fibronectin matrix was deposited by cells attached to the hybrid ECM scaffold than to the scaffold alone (compare A and B with D and E). Note that the fibers remain intact throughout the 7 d culture (C, F). Scale bar = 50  $\mu\text{m}$ .